Chapter 7

Spatial Distribution of Aerosol Optical Thickness Retrieved from SeaWiFS Images by a Neural Network Inversion over the West African Coast

Daouda Diouf, Awa Niang, Julien Brajard,
Salam Sawadogo, Michel Crepon and Sylvie Thiria

Additional information is available at the end of the chapter

http://dx.doi.org/10.5772/65874

Abstract

Aerosol optical thickness (AOT) was provided by SeaWiFS over oceans from October 1997 to December 2010. Weekly, monthly, and annually maps might help scientifics to better understand climate change and its impacts. Making average of several images to get these maps is not suitable on West African coast. A particularity of this area is that it is constantly traversed by desert dust. The algorithm used by SeaWiFS inverts the reflectance measurements to retrieve the aerosol optical thickness at 865 nm. For the poorly absorbing aerosol optical thickness less than 0.35, the standard algorithm works very well. On the west African coast that is often crossed by desert aerosol plumes characterized by high optical thicknesses. In this paper we study the spatial and temporal variability of aerosols on the West African coast during the period from December 1997 to November 2009 by using neural network inversion. The neural network method we used is mixed method of neuro-variational inversion called SOM-NV. It is an evolution of NeuroVaria that is a combination of a variational inversion and multilayer perceptrons, multilayer perceptrons (MLPs). This work also enables validation of the optical thickness retrieved by SOM-NV with AOT in situ measurements collected at AErosol RObotic NETwork (AERONET) stations.

Keywords: West African coast, absorbing aerosols, neural networks

1. Introduction

The sensor SeaWiFS ocean color provides daily luminance measurements of ocean-atmosphere system in the visible and near infrared since October 1997. Luminances are at wavelengths 412,

443, 490, 510, 555, 670, 765, and 865 nm. For each wavelength λ, the TOA reflectance ρ is computed as

$$\rho(\lambda, \theta_V, \phi) = \frac{\pi \cdot L(\lambda, \theta_V, \Delta\Phi)}{E_0(\lambda) \cdot \cos(\theta_S)} \tag{1}$$

where $E_0(\lambda)$ is the extraterrestrial solar irradiance (in Wm^{-2} nm^{-1}, varying with the sun-earth distance), θ_s and θ_v are the sun- and satellite-viewing zenith angles, respectively, and $\Delta\Phi = \phi_o - \phi_v$ is the azimuth angle difference between the satellite and the sun.

SeaWiFS aerosol products are generated, validated, and made available by NASA. These aerosols from the standard atmospheric correction algorithm can hardly be used for global aerosol studies because of aerosol optical thickness greater than about 0.35.

Plumes of absorbing aerosols are observed regularly on the West African coast near the Sahara, which prevents spatial and temporal operation of atmospheric and oceanic parameters.

This paper presents a new method to retrieve the aerosol parameters from ocean color satellite radiometer and is able to give information on absorbing aerosols.

2. Data and method

For this study, we use daily luminance measurements made by the SeaWiFS sensor off the West African coast in an area between 8°–24°N and 14°–30°W. These measures extend the period of 1997–2009. The TOA reflectance ρ is the sum of contributions to the signal of each constituent of the atmosphere and ocean. The contribution of Rayleigh scattering, specular reflection, and absorption gas is known a priori with accuracy and has been removed from the signal. The pixels of clouds have been removed using the cloud detection algorithm [1]. Thus, the corrected reflectance is

$$\boldsymbol{\rho}_{used} = \boldsymbol{\rho}_a + \boldsymbol{\rho}_{ra} + t\boldsymbol{\rho}_w \tag{2}$$

where $\rho_a + \rho_{ra}$ is the atmospheric contribution, ρ_w is the contribution of the water, and t is the transmittance of the atmosphere at a given wavelength (λ).

We used satellite data sets comprising ten-dimensional vectors, whose components are eight wavelengths measured by the radiometer and two viewing angles since the reflectance spectra depend on the geometry of the measurement. These angles are the sun zenith angle θ_s, and the scattering angle γ is defined as

$$\gamma = \arccos(-\cos\theta_v \cos\theta_s + \sin\theta_v \sin\theta_s \cos\Delta\Phi) \tag{3}$$

Each vector, whose components correspond to the SeaWiFS wavelengths, represents a ρ_{used} spectrum.

http://dx.doi.org/10.5772/65874

The learning dataset $Data^{obs}$ consists of ρ_{used}^{obs} observed at eight wavelengths (412, 443, 490, 510, 555, 670, 765, and 865 nm) extracted from pixels of SeaWiFS images during the year 2003 and two associated viewing angles (i.e., the sun zenith angle θ_s and the scattering angle γ). $Data^{obs}$ is thus composed of ten-component vectors.

We also used theoretical database $\text{Data}^{\text{expert}}$ that consists of the ρ_{used}^{expert} computed at eight wavelengths with a 2-layer radiative transfer model [2] for various optical thickness values, chlorophyll content, and geometry of the measurement and for five aerosol models.

Each $\text{Data}^{\text{expert}}$ vector comprises eight spectral components (ρ_{used}^{expert}) and two geometry components which are the sun zenith angle θ_s and the scattering angle γ. $\text{Data}^{\text{expert}}$ comprises 12,000,000 simulated vectors using four aerosol models (maritime, oceanic, coastal, and tropospheric) [3] and one absorbing aerosol (African dusts) [1]. The five aerosol models were computed at four different relative humidity (70%, 80%, 90%, and 99%).

$\text{Data}^{\text{expert}}$ was used in order to introduce the expertise and to retrieve the aerosol type and the optical thickness values.

In this study, we used SOM-NV [2], a two successive statistical models for analyzing the $Data^{obs}$ images: the self-organizing map (SOM) [4] model and the NeuroVaria method [5, 6]. We first processed the images with a SOM model, which is well suited for visualizing and clustering a high-dimensional data set. We denoted this topological map as SOM-Angle-Spectrum (SOM-A-S). In the light of the results obtained by Niang et al. [7], we chose a similar architecture for SOM-A-S, a two-dimensional array with a large number of neurons (20 × 30 = 600). SOM-A-S was learned on the $Data^{obs}$ of the year 2003. The vectors of the learning data set were thus clustered into 600 groups, allowing a highly discriminative representation of $Data^{obs}$. The second dataset, $Data^{expert}$, representing the expertise, was used to decode the SeaWiFS images. The principle of the method is to compare the ten-component vectors of $Data^{expert}$ whose associated parameters are known, with those of the neurons of SOM-A-S according to a distance. At the end of the labeling, each neuron of SOM-A-S map has captured a set of ρ^{expert} and takes a label, which is extracted from that set according to the procedure described in [7]. Each neuron is therefore associated with an atmospheric and ocean physical parameters (τ (AOT: aerosol optical thickness), C (*chlorophyll-a pigment*)), and an aerosol type. The SOM-A-S map being labeled, we are able to analyze a satellite image by projecting the ten-component vector (reflectances and viewing angles) associated with each pixel on the SOM-A-S map. Pixels captured by a neuron are assigned to the aerosol type and optical thickness associated with this neuron. For monthly climatology images, the aerosol type is estimated as the median of the types of the images considered.

The second statistical model improves the retrieval of the optical thickness. We used a neuro-variational algorithm called NeuroVaria that is able to provide accurate atmospheric corrections for inverting satellite ocean color measurements. The algorithm minimizes a weighted quadratic cost function, J, by adjusting control parameters (atmospheric and oceanic) such as τ and C [8]. J describes the difference between the satellite measurement $\rho_{toa}^{mes}(\lambda)$ $\boldsymbol{\rho}^{obs}$ and a simulated reflectance $\rho_{toa}^{sim}(\lambda)\rho^{sim}$ computed using radiative transfer codes modeled by

supervised neural networks (the so-called multilayer perceptrons, MLPs). The minimization implies the computation of the gradient of J with respect to the control parameters and consequently of the derivatives of the MLPs, which is done by the classical gradient back-propagation algorithm [9]. On this version of SOM-NV, the MLPs modeling the radiative transfer codes were specially designed to take African dusts into account.

A major advantage of the method is a gain in number of processed pixels from SeaWiFS. This work also enables validation of the optical thickness retrieved by SOM-NV with in situ measurements of optical thicknesses AERONET collected at stations in Dakar and Cabo Verde [2].

The complete methodology was applied to SeaWiFS images of the ocean off the West African coast from 1997 to 2009 to produce the type of aerosol, the aerosol optical thickness, and the chlorophyll-a concentration.

Monthly mean map aerosols and chlorophyll-a were calculated on 9 km × 9 km used for SeaWiFS GAC product level 3. Seasonality strong $\tau(865)$ is characterized by a strong invasion of dust into the months of June, July, and August. Their intensities vary from year to year, depending on aridity conditions in Africa and the wind direction.

3. Results

In **Figure 1**, we compare for each pixel of the image (March 10, 2004), the optical thickness and *Chl-a* concentration given by SeaWiFS algorithm (column 2) and those retrieved with SOM-NV (column 1). More than half are fully covered by Saharan dust with high optical thickness in these parts. In most standard SeaWiFS algorithm, a wide area of the image is not processed, while the satellite image can clearly observe the absorbing aerosol event. The SeaWiFS algorithm does not

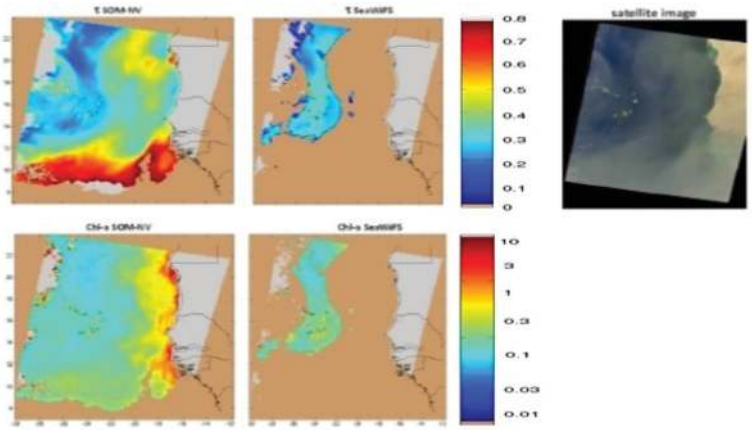

Figure 1. Image of March 10, 2004; the first column represents the SOM-NV processing and the second the SeaWiFS processing. The last column represents the RGB satellite image.

http://dx.doi.org/10.5772/65874

generally process Saharan dust (see image in "true" colors); these absorbing Saharan dust are generally characterized by high optical thickness. The SOM-NV method permits retrieval of the aerosol type and aerosol optical properties from the statistical properties of the data. These retrievals are accurate for optical thickness values higher than 0.35. This is not the case for the standard SeaWiFS product. This permitted us to dramatically increase the number of pixels processed with respect to the standard SeaWiFS algorithm by an order of magnitude.

Maps of average aerosol and chlorophyll-a were computed on grids of 9 km × 9 km GAC used for SeaWiFS level-3 GAC products. The averages obtained by SOM-NV seem statistically more representative than those obtained by SeaWiFS. Monthly averages of optical thickness obtained by the standard processing for the months of March and June of **Figure 2** are drastic because only τ values not exceeding 0.35 are taken into account. These failures demonstrate impossibility for SeaWiFS to establish spatial and temporal global maps of aerosol particularly in absorbing area. This is due to the fact that desert aerosols frequently cross the ocean [10] preventing the standard algorithm to retrieve these aerosols and chlorophyll-a below them.

In **Figure 3**, average of AOT (top), Chl-a (middle) of the months of January and April 2005 is shown. As seen in **Figure 2**, we note also in **Figure 3** failure for SeaWiFS to establish consistent spatial and temporal global maps of aerosol optical thickness. Fluctuations in the chlorophyll-a observed at **Figure 3** are the same in the image for both algorithms. In terms of intensity, the values of Chl-a are higher for the standard algorithm at the continental shelves. An intercomparison with the SeaWiFS standard processing showed that the SOM-NV methodology increased the number of pixels processed of a factor until 10. This is due to the impossibility of the standard algorithm to retrieve the chlorophyll-a in the presence of Saharan dust, which frequently cross the ocean. The low number of pixels processed by SeaWiFS may bias the mean chlorophyll-a maps.

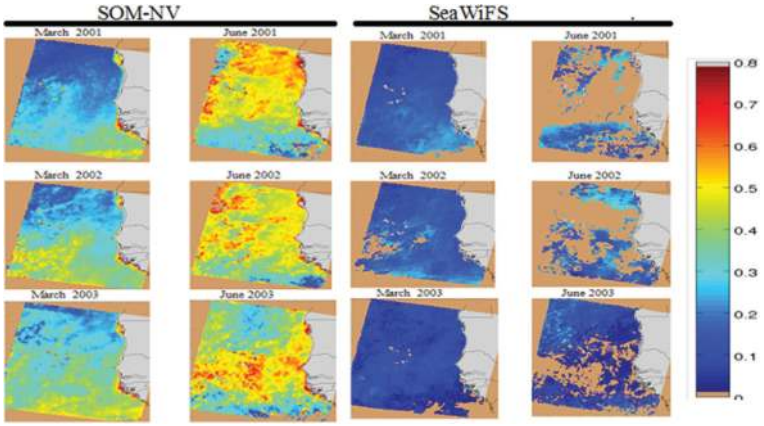

Figure 2. Spatial distribution of the aerosol optical thickness. Monthly average in March and June of the years 2001, 2002, and 2003. We note the same trends from 1 year to another. The aerosol optical thickness are strong in June and relatively low during the month of March for the SOM-NV processing (*left block*) and very low for the standard processing (*right block*).

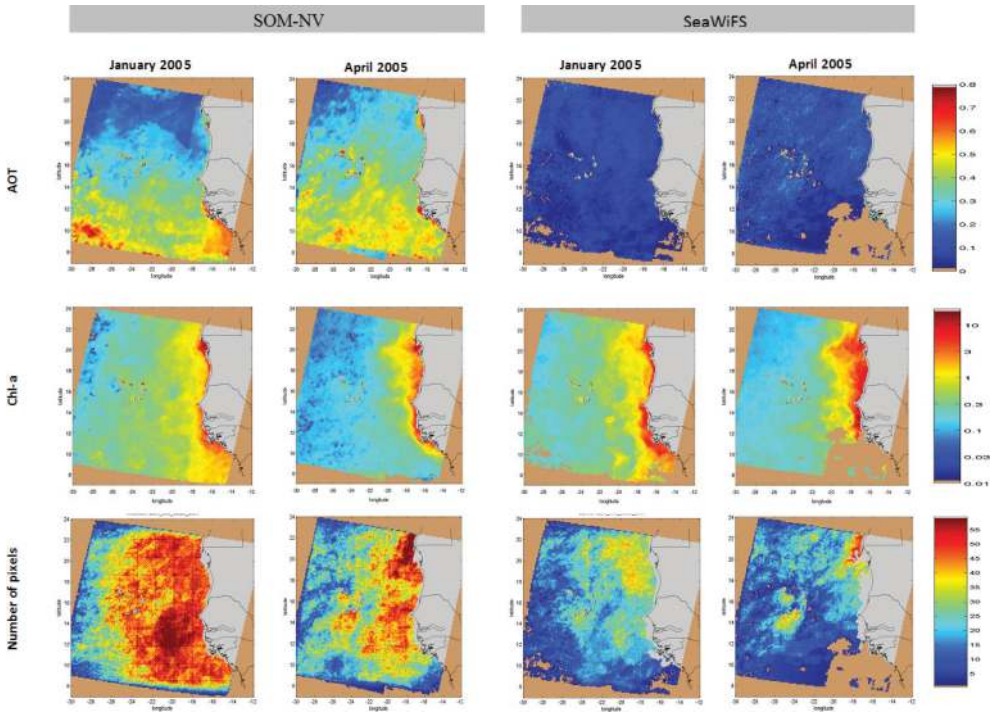

Figure 3. Average of AOT (*top*), Chl-a (*middle*) of the months of January and April 2005 and the number of pixels used in calculating the average (*bottom*).

The presence of the case 2 waters explains these high values of Chl-a. The hypothesis of dark ocean is no longer valid in case of water 2. These results confirm that atmospheric corrections on the Saharan dust by SOM-NV are correct because Chl-a retrievals using OC4V4 are satisfactory spatial and in intensity.

Direct measurements of the optical thickness at 865 nm $\tau(865)$ were performed at two ground stations (Dakar-M'Bour—14°24N and 16°58W and Cabo Verde-Sal Island—16°45N and 22°57W). These measurements were made in the framework of the AErosol RObotic NETwork (AERONET) program which is a federated international network of sun/sky radiometers [11, 12]. Level 2.0 sun photometer measurements $Data^{photometer}$ (cloud screened and quality assured) at the two ground stations are available from 1998 to 2009.

The two AERONET measurements are found when at least one half of the SeaWiFS, or the SOM-NV retrievals within a 5 × 5 pixels square box containing the AERONET site are valid. The AERONET optical thickness values used for this validation were actually the mean of all the measurements made between 12:00 UT and 14:00 UT, because SeaWiFS images over the area were taken around 13:00 UT. We computed mean value for each month.

http://dx.doi.org/10.5772/65874

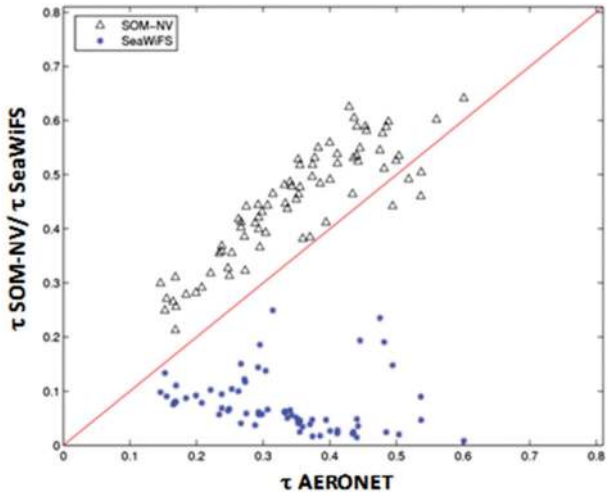

Figure 4. Scatter plot between monthly mean optical thickness measurements computed by SOM-NV (Δ) and the SeaWiFS product (*) and the AERONET measurement at Dakar.

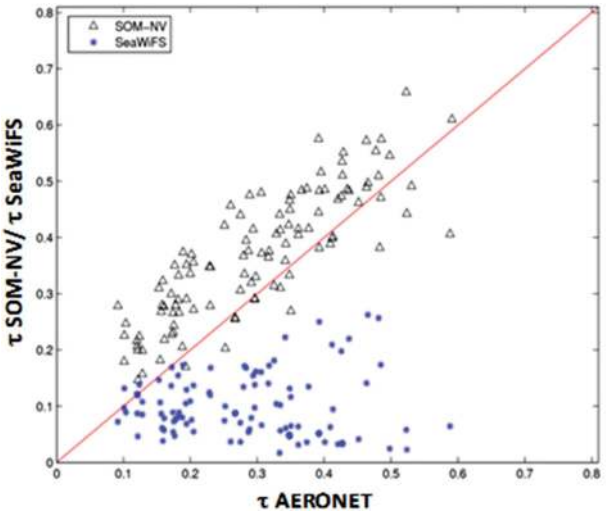

Figure 5. Scatter plot between monthly mean optical thickness measurements computed by SOM-NV (Δ) and the SeaWiFS product (*) and the AERONET measurement at Cabo Verde.

	SOM-NV	**SeaWiFS**
Mean relative error	38.8%	74.54%
Correlation	80.23	13.45%

Table 1. The performance indicators in Dakar site.

	SOM-NV	SeaWiFS
Mean relative error	40.5%	74.75%
Correlation	82.34%	6.38%

Table 2. The performance indicators in Cabo Verde site.

Figures 4 and **5** confirm that the mean aerosol maps shown above in **Figure 2** are better for SOM-NV than SeaWiFS.

We compared the root-mean-square error (RMSE) and the mean relative error (MRE) of $\tau^{SOM\text{-}NV}$ and τ^{SeaW} with respect to the observed τ^{AERO}.

The MRE remains low for SOM-NV (38.8% at Dakar, 40.5% at Cabo Verde), the RMSE are less than 0.03, and the correlations are 80.23% at Dakar station and 82.34% at Cabo Verde. However, for SeaWiFS, the correlation is 13.45% for Dakar and 6.38% for Cabo Verde, and the MRE is 74.54% at Dakar and 60.75% at Cabo Verde. These results are resumed in **Tables 1** and **2**.

4. Conclusion

SOM-NV, an original and efficient method to retrieve optical properties from TOA reflectance measured by satellite-borne multispectral ocean color sensors, has permitted to study realistic spatial distribution of aerosol optical thickness and chlorophyll-a. The method is based on a combination of a neural network classification and a variational optimization. It makes use of the full spectrum of measurements to perform the aerosol identification. The means obtained by SOM-NV appear statistically more representative than those obtained by SeaWiFS. Monthly mean of aerosol optical thicknesses obtained by the standard processing for March and June are drastic because only τ values not exceeding 0.35 are considered. These temporal and spatial failures demonstrate the impossibility of establishing by SeaWiFS global maps of aerosols especially in absorbing environment. The number of pixels processed by SOM-NV even double or triple those computed by SeaWiFS. This is due to the fact that desert aerosols frequently cross the ocean preventing the standard algorithm to retrieve these aerosols and chlorophyll-a below them.

Author details

Daouda Diouf[1]*, Awa Niang[1], Julien Brajard[2], Salam Sawadogo[1], Michel Crepon[2] and Sylvie Thiria[2]

*Address all correspondence to: dadiouf2001@yahoo.fr

1 Ecole Supérieure Polytechnique, Université Cheikh Anta Diop de Dakar, Dakar Fann, Sénégal

2 IPSL/LOCEAN, Université, Paris, France

http://dx.doi.org/10.5772/65874

References

[1] Moulin, C., Gordon, H. R., Banzon, V. F., & Evans, R. H. (2001). Assessment of Saharan dust absorption in the visible from SeaWiFS imagery. Journal of Geophysical Research, 106, 18239–18250.

[2] Diouf, D., Niang, A., Brajard, J., Crepon, M. and Thiria, S. (2013). Retrieving aerosol characteristics and sea-surface chlorophyll from satellite ocean color multi-spectral sensors using a neural-variational method. Remote Sensing of Environment, 130, ISSN: 0034-4257, 74–86. DOI:10.1016/j.rse.2012.11.002.

[3] Shettle, E. P. & Fenn, R. W. (1979). Models of aerosols of the lowers atmosphere and the effect of the humidity variations on their optical properties. Technical Report TR-79-0214, Air Force Geophysical Laboratory, Bedford, Mass.

[4] Kohonen, T. (2001). Self organizing maps (3rd ed.). Berlin Heidelberg: Springer Verlag. 501 pp.

[5] Brajard, J., Jamet, C., Moulin, C. and Thiria, S. (2006). Use of a neuro-variational inversion for retrieving oceanic and atmospheric constituents from satellite ocean colour sensor: application to absorbing aerosols. Neural Networks 19, 178–185.

[6] Jamet, C., Thiria, S., Moulin, C., & Crepon, M. (2005). Use of a neuro-variational inversion for retrieving oceanic and atmospheric constituents from ocean color imagery. A feasibility study. Journal of Atmospheric and Oceanic Technology, 22, (4), 460–475. Doi:10.1175/JTECH1688.1

[7] **N**iang, A., Badran, F., Moulin, C., Crépon, M. & Thiria, S. (2006). Retrieval of aérosol type and optical thickness over the Mediterranean from SeaWiFS images using an automatic neural classification method. Remote Sensing of Environment, 100, 82–94.

[8] Brajard, J., Niang, A., Sawadogo, S., Fell, F., Santer, R. and Thiria, S.. (2007). Estimating aerosol parameters from MERIS ocean colour sensor observations by using topological maps. International Journal of Remote Sensing, 28, 3–4, 781–795.

[9] Bishop, C. (1995). Neural networks for pattern recognition. Oxford University Press, Inc. New York, NY, USA ISBN:0198538642

[10] Nobileau, D. & Antoine, D. (2005). Detection of blue-absorbing aerosols using near-infrared and visible (ocean color) remote sensing observations. Remote Sensing of Environment, 95, 368–387.

[11] Holben, B., Eck, T., Slutsker, I., Tanre´, D., Buis, J. P., Setzer, E., et al. (1998). AERONET—a federated instrument network and data archive for aerosol characterization. Remote Sensing of Environment, 66, 1–16.

[12] Tanre, D., Deroo, C., Duhaut, P., Herman, M., Morcrette, J., Perbos, J. and Deschamps, P. J. (1997). Description of a computer code to simulate the satellite signal in the solar spectrum: 5s code. International Journal of Remote Sensing, 11, 659–668